Article published online: 2024-05-23

Design, Synthesis, and Evaluation of Novel Cryptotanshinone Derivatives for Activity against Triple-Negative Breast Cancer

Siyu Liu[1] Panpan Zhang[1] Qingyan Sun[1]*

[1] National Key Laboratory of Lead Druggability Research, Shanghai Institute of Pharmaceutical Industry Co., Ltd., China State Institute of Pharmaceutical Industry Co., Ltd., Shanghai, People's Republic of China

Pharmaceut Fronts 2024;6:e136–e148.

Address for correspondence Qingyan Sun, PhD, National Key Laboratory of Lead Druggability Research, Shanghai Institute of Pharmaceutical Industry Co., Ltd., China State Institute of Pharmaceutical Industry Co., Ltd., 285 Gebaini Road, Shanghai 201203, People's Republic of China (e-mail: sqy_2000@163.com).

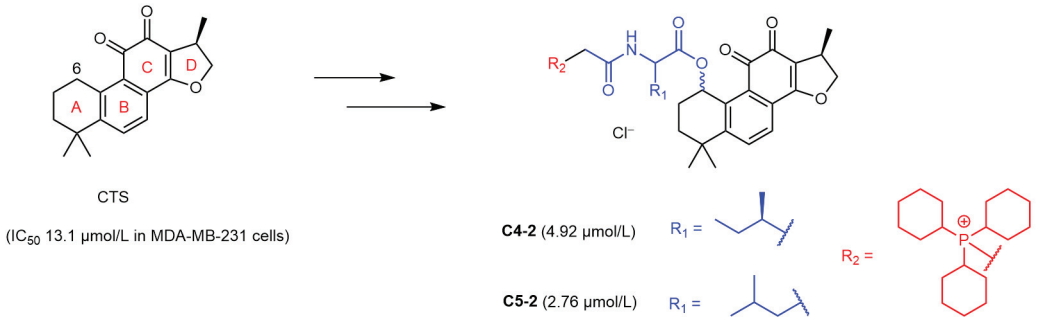

Abstract

Triple-negative breast cancer (TNBC) can be difficult to treat because of resistance to existing therapeutic agents. Our prior studies revealed the inhibitory effect of the natural product cryptotanshinone (CTS) on the proliferation of TNBC cells; however, its clinical application was prevented due to its low water solubility and activity. This study aimed to synthesize derivatives of CTS with enhanced potency and water solubility. The structure of CTS was modified by adding amino acid side chains, which were derived into phosphonium salts. The derivatives were immersed in phosphate-buffered saline (PBS) to assess their water solubility. The antitumor effects of the derivatives against MDA-MB-231 breast cancer cells were assessed by evaluating their roles in regulating cell proliferation, cell apoptosis, and cell-cycle arrest using cell counting kit-8 (CCK-8), flow cytometry, and calcein-AM/propidium iodide assay, respectively. In this work, a total of 29 derivatives of CTS were synthesized, of which the tricyclohexylphosphine derivatives **C4-2** and **C5-2** were highly soluble in PBS, with 790- and 450-fold higher than that of CTS, respectively, and at the same time, the antitumor activities of **C4-2** and **C5-2** were also enhanced, with two- and fourfold higher than that of CTS, respectively. Further studies revealed that the compounds may inhibit the proliferation of MDA-MB-231 by inducing cellular arrest in the G2/M phase. These findings provided preliminary data for the mechanisms of CTS and its derivatives in blocking TNBC and suggested **C4-2** and **C5-2** as potential agents for the treatment of the disease in the future.

Keywords

- triple-negative breast cancer
- cryptotanshinone
- derivatives

received
September 18, 2023
accepted
March 23, 2024
article published online
May 23, 2024

DOI https://doi.org/10.1055/s-0044-1786032.
ISSN 2628-5088.

Georg Thieme Verlag KG, Rüdigerstraße 14, 70469 Stuttgart, Germany

Introduction

Breast cancer is an extremely common malignant tumor in women and the second leading cause of cancer-related mortality in women.[1] Breast cancer can be classified into five molecular subtypes based on the expression status of hormone receptors, of which triple-negative breast cancer (TNBC) accounts for 15 to 20% of all breast cancers, and is the only breast cancer subtype that lacks effective targeted therapies because it does not express estrogen receptor (ER), progesterone receptor, and epidermal growth factor receptor 2. TNBC is characterized by a high metastatic rate, low survival rate, and poor prognosis,[2] and the current systemic therapy relies on chemotherapy with paclitaxel- and anthracycline-containing drugs. However, studies have revealed that TNBC has become resistant to the existing chemotherapeutic agents.[3]

Natural products are characterized by diverse structures, diverse biological activities, low toxicity, and wide availability, and play an essential role in the development of new drugs.[4] In this work, we focused on natural products in an attempt to identify new lead compounds with potential anticancer properties for further optimization. Cryptotanshinone (CTS), a fat-soluble compound extracted from the roots and rhizomes of *Salvia miltiorrhiza*, has been found to exhibit anticancer, anti-inflammatory, immunomodulatory, neuroprotective, and antifibrotic activities.[5] CTS inhibits breast carcinoma growth and induces apoptosis by competitively binding to ER, stimulating the immune system through the JAK2/STAT4 pathway, and causing endoplasmic reticulum stress.[6–8] Unfortunately, CTS has poor water solubility and low bioavailability for oral administration. The water solubility of CTS is only 9.76 g/mL,[9] the absolute oral bioavailability in rats is 2.05%.[10] For pigs, when 40 mg/kg of CTS was given orally, only 0.043 mg/kg was detected 1 hour after administration.[11]

In the present study, an attempt was made to explore a series of derivatives of CTS with enhanced antitumor activity and water solubility. The chemical structure of CTS is shown in ►**Fig. 1**. Structure–function relationship analyses showed that the *o*-dicarbonyl group of the C-ring is a key group for the efficacy of CTS, and destroying the group decreases the activity of the drug. CTS has a similar chemical structure to tanshinone IIA, except that the D-ring of CTS has one less double bond. The D-ring of CTS is less reactive and cannot undergo substitution, addition, or oxidation reactions of the double bond.[12] Zhang et al and Ding et al reported the selective and direct introduction of various acyl and phenolic groups into the C-6 position of the A-ring, which fueled substantial research on the A-ring.[13,14] On this basis, Bi's group reported the introduction of aromatic acid derivatives or phenolic units at the C-6 position, and screened the resulting compounds for vasodilatory and cardioprotective activities, and identified derivatives with comparable or better activities than CTS.[15,16] These preceding studies provided valuable information for further structural modification, however, the roles of modification at the C-6 position of CTS on antitumor activity remained largely unknown.

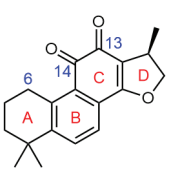

Fig. 1 CTS chemical structure. CTS, cryptotanshinone.

In this work, the structure of the CTS was modified in two aspects. First, an amino acid group was introduced at the C-6 position to reduce toxicity, improve targeting and selectivity to tumor cells, and increase the water solubility of the agent. Second, the introduced amino acid reacts with triphenylphosphine or tricyclohexylphosphine to generate quaternary phosphonium salts to improve the water solubility again. The CTS derivatives were initially screened by determining the effects of derivatives of CTS on the proliferation of TNBC cells (MDA-MB-231) using a cell counting kit-8 (CCK-8) method, followed by a preliminary structure–function relationship analysis. For the screened compounds, flow cytometry and cell staining were conducted to investigate *in vitro* antitumor activity of the compounds.

Results and Discussion

Synthesis of CTS Derivatives

The introduction of hydrophilic or ionized groups is a common strategy to improve water solubility. Generally, the available hydrophilic groups are chain or cyclic groups containing nitrogen and oxygen atoms, whereas amino acids, as the basic components of cell structure, have the advantages of low toxicity, structural diversity, and potential targeting of carrier-mediated transport proteins. According to the structural features of CTS, the sp^3 hybridized carbon at the benzyl position of the A-ring can be used as the reaction site for conjugate addition. To this end, chloroacetyl-substituted amino acids with different substituents and lengths were selected for the reaction without altering the structure of the CTS backbone, and 11 amino acid derivatives were synthesized (**A1–A6-2**, ►**Scheme 1**). During a 1,6-conjugate addition reaction of an amino acid with a carbon at the C-6 position, the methylene group at the C-6 position can form a dienone conjugation system with the C-13 and C-14 positions of the C-ring. Negative ions of the carboxylic acid group in the amino acid structure can attack the C-6 position from the upper and lower directions of the conjugation plane, enabling the generation of two 1,6-conjugate addition products with different configurations. However, the degree of separation of the two diastereoisomers increases as the size of the side-chain substituents of the amino acids increases. Several pairs of diastereoisomers have been successfully isolated (e.g., **A2-1** and **A2-2**, **A3-1**, and **A3-2**) in this work; unfortunately, various methods failed to reveal the conformations of the diastereoisomers. To obtain derivatives with enhanced water solubility, triphenylphosphine or tricyclohexylphosphine is susceptible to nucleophilic attack on chlorine-bonded carbon atoms, resulting in the generation of 18 phosphonium salt derivatives (**B1–B6**, **C1–C6-2**, ►**Scheme 1**). The changes in

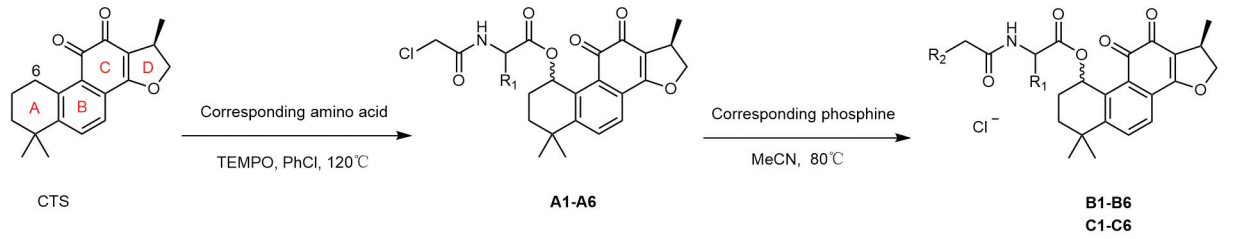

	R_1		R_1	R_2		R_1	R_2
A1**	H	**B1****	H	(PPh_3)	**C1****	H	(TCHP)
A2-1*	$-CH_3$	**B2-1***	$-CH_3$	PPh_3	**C2-1***	$-CH_3$	TCHP
A2-2*	$-CH_3$	**B2-2***	$-CH_3$	PPh_3	**C2-2***	$-CH_3$	TCHP
A3-1*		**B3-1***		PPh_3	**C3-1***		TCHP
A3-2*		**B3-2***		PPh_3	**C3-2***		TCHP
A4-1*		**B4**		PPh_3	**C4**		TCHP
A4-2*		**B5**		PPh_3	**C5-1***		TCHP
A5-1*		**B6**		PPh_3	**C5-2***		TCHP
A5-2*					**C6-1***		TCHP
A6-1*					**C6-2***		TCHP
A6-2*							

Scheme 1 Synthetic routes of the derivatives of CTS. CTS, cryptotanshinone. Note: -1* and -2* have the same structure, but the configuration of **C-6** is opposite; the symbol "**" denotes a mixture of -1 and -2.

the water solubility and anti-TNBC activity were investigated by comparing the changes of amino acids and phosphine groups among the derivatives.

Primary Screening of the Derivatives of CTS with Antiproliferative Activity

The CCK-8 assay was used to investigate the effects of the derivatives on MDA-MB-231 cell proliferation at low, medium, and high concentrations (0.3, 3, and 30 μmol/L). A study of structure–function relationships was conducted to screen the preferred derivatives. As shown in **Table 1**, in comparison to the lead compound, the amino acid derivatives (except **A3-1**) displayed stronger cytotoxicity against MDA-MB-231 cells at a high concentration (30 μmol/L), strikingly, most of the phosphonium salt derivatives further enhanced the cytotoxicity at a medium concentration (3 μmol/L) compared to the amino acid derivatives, suggesting the feasibility of introducing hydrophilic groups to improve the LogP to enhance the activity of the lead compound. Among the derivatives, **C4-2** and **C5-2** displayed the best activities with IC_{50} values being 4.92 and 2.76 μmol/L, respectively (►**Fig. 2**), and were two- and fourfold greater cytotoxicity than CTS ($IC_{50} = 13.11$ μmol/L),[17] respectively. Thus, **C4-2** and **C5-2** were chosen for the subsequent study.

C4-2 and C5-2 Induce Apoptosis in MDA-MB-231 Cells

MDA-MB-231 cells were treated with different concentrations of **C4-2** and **C5-2** (0.3, 1, 3, 10, 30 μmol/L), then cell apoptosis was evaluated. As shown in ►**Fig. 3**, **C4-2** and **C5-2** significantly increased the percentage of necrotic cells, as indicated by red fluorescence attributable to propidium

Table 1 Effect of different concentrations of derivatives of CTS on the survival of MDA-MB-231 cells

Compd.	Cell viability (%)		
	0.3 μmol/L	3 μmol/L	30 μmol/L
CTS	86.95 ± 6.86	68.95 ± 6.114	7.90 ± 1.40
A1**	105.25 ± 3.97	109.46 ± 3.29	3.97 ± 0.35
A2-1*	105.59 ± 3.54	108.60 ± 8.23	3.35 ± 0.42
A2-2*	104.72 ± 4.41	109.69 ± 0.69	3.21 ± 0.45
A3-1*	119.43 ± 8.08	116.59 ± 3.09	9.56 ± 0.59
A3-2*	91.48 ± 6.13	98.23 ± 4.37	3.12 ± 0.41
A4-1*	103.96 ± 9.36	108.07 ± 10.62	5.52 ± 0.60
A4-2*	104.33 ± 5.57	116.21 ± 5.30	4.51 ± 0.37
A5-1*	108.45 ± 5.68	106.59 ± 2.69	3.60 ± 0.56
A5-2*	92.55 ± 8.32	92.83 ± 9.40	2.32 ± 0.27
A6-1*	100.48 ± 0.94	100.99 ± 7.09	5.54 ± 0.63
A6-2*	95.89 ± 6.46	99.90 ± 1.09	5.09 ± 0.30
B1**	99.82 ± 2.96	71.88 ± 5.20	5.35 ± 0.29
B2-1*	129.59 ± 0.73	78.79 ± 5.84	7.75 ± 0.86
B2-2*	121.11 ± 6.17	80.53 ± 4.43	54.17 ± 2.28
B3-1*	118.42 ± 1.13	91.40 ± 6.15	9.37 ± 0.38
B3-2*	110.36 ± 4.58	94.05 ± 3.69	9.37 ± 1.42
B4-1	100.08 ± 1.68	86.58 ± 3.69	10.17 ± 0.69
B5-1	110.88 ± 2.84	94.15 ± 0.64	89.08 ± 2.63
B6-1	94.91 ± 2.41	108.84 ± 4.79	80.85 ± 3.70
C1**	92.02 ± 3.61	100.93 ± 6.26	2.38 ± 0.12
C2-1*	108.90 ± 3.47	71.32 ± 1.45	9.46 ± 0.78
C2-2*	107.15 ± 2.10	105.19 ± 2.70	7.87 ± 0.68
C3-1*	123.06 ± 6.64	116.85 ± 4.26	8.07 ± 1.47
C3-2*	102.77 ± 5.08	78.67 ± 5.48	7.09 ± 0.99
C4-1*	104.15 ± 8.49	71.38 ± 2.74	12.48 ± 1.14
C4-2*	93.70 ± 4.22	19.68 ± 1.79	15.38 ± 1.35
C5-1*	99.07 ± 6.18	77.87 ± 2.97	10.02 ± 0.61
C5-2*	84.62 ± 2.44	40.33 ± 2.35	13.83 ± 4.79
C6-1*	103.14 ± 4.70	76.01 ± 2.91	9.19 ± 0.64
C6-2*	101.37 ± 7.20	81.41 ± 4.47	6.94 ± 1.57

Abbreviation: CTS, cryptotanshinone.
Note: -1* and -2* have the same structure, but the configuration of **C-6** is opposite; the symbol "**" denotes a mixture of -1 and -2.

iodide (PI) uptake compared to the control, and the effect was more pronounced, especially at high concentrations (10, 30 μmol/L). The extent of red fluorescence, which reflects the intracellular DNA content, increased with increasing concentrations of **C4-2** and **C5-2**, suggesting the pro-apoptotic effect of the compound in a dose-dependent manner.

C4-2 and C5-2 Induce Cell-Cycle Arrest in MDA-MB-231 Cells

Flow cytometry was performed to investigate the effect of **C4-2** and **C5-2** on cell growth cycle. As shown in ►**Fig. 4A**, **C4-2** (0.3 μmol/L) induced 65.10% of cells in the G0/G1 phase, 10.89% in the S phase, and 22.36% in the G2/M phase. However, **C4-2** (1 μmol/L) and **C4-2** (3 μmol/L) decreased the proportion of cells in the G0/G1 phase to 64.39 and 52.77%, and increased the proportion of cells in the S phase to 11.36 and 15.27%, and G2/M phases to 22.77 and 30.18%, respectively. **C4-2** blocks cell-cycle progression at G0/G1 in MDA-MB-231 cells in a dose-dependent manner, and the subsequent cell cycle at G2/M, which may contribute to the growth inhibitory effect of the compounds on MDA-MB-231 cells. When the cells were treated with **C5-2** (0.3, 1, 3 μmol/L), similar change treads were also observed (►**Fig. 3B**).

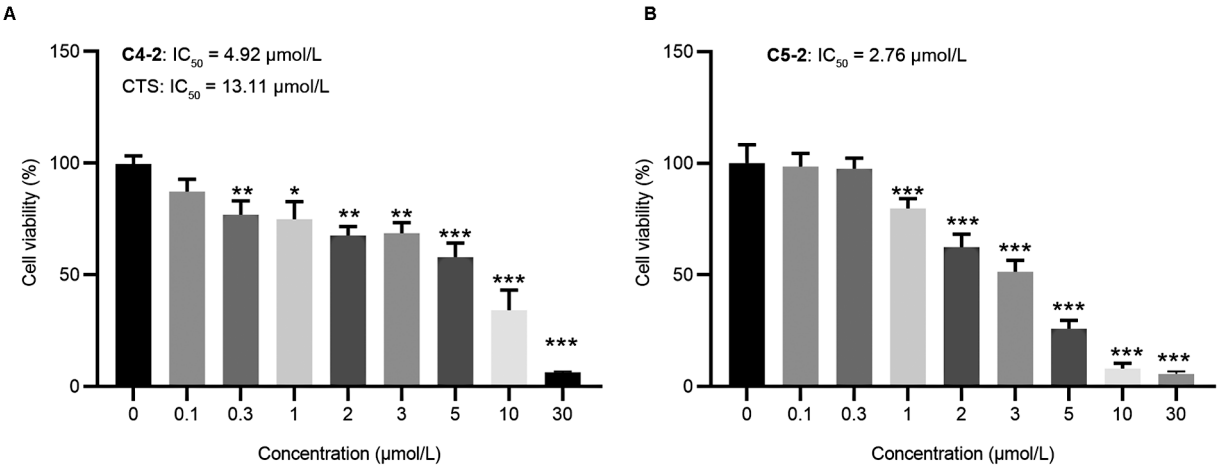

Fig. 2 Proliferation of MDA-MB-231 cells exposed to (**A**) **C4-2** and (**B**) **C5-2**. $^{**}p \leq 0.01$, $^{***}p \leq 0.001$ versus the proliferation of MDA-MB-231 cells without drug treatment.

C4-2 and C5-2 Kill MDA-MB-231 Cells

MDA-MB-231 cells were treated with different concentrations of **C4-2** and **C5-2**. AM/PI live/dead cell staining was performed to visualize the process of cell death. As shown in ►**Fig. 5** (**A** and **B**), in comparison to the control, **C4-2** and **C5-2** decreased the number of live cells, whereas increased the number of dead cells in a dose-dependent manner with the maximum effect being observed at 10 μmol/L, confirming the killing ability of **C4-2** and **C5-2** on MDA-MB-231 cells.

Water Solubility of the C4-2 and C5-2

Water solubility is an essential feature in the formation of small-molecule drugs, and an agent with poor water solubility is often associated with low bioavailability. In this work, **C4-2**, **C5-2**, and their synthetic precursors (**A4-2** and **A5-2**) were selected for the determination of the water solubility in phosphate-buffered saline (PBS). As shown in **Table 2**, the solubilities of **A4-2**, **A5-2**, **C4-2**, and **C5-2** were more than 100-fold higher than those of CTS. Particularly, the solubility of **C4-2** and **C5-2** in PBS reached 172.585 and 99.659 μg/mL, respectively, which were approximately 790- and 450-fold higher than that of CTS, respectively, confirming the success of our modification strategy in improving the water solubility of the derivatives of CTS.

Conclusion

In this study, CTS was used as a lead compound to obtain derivatives with improved water solubility and biological activity by introducing amino acid side chains and phosphine salts at the C-6 position. Among the derivatives, tricyclohexylphosphine-derived **C4-2** and **C5-2** were 790- and 450-fold more soluble than CTS, respectively, and 2- and 4-fold more active than CTS in inhibiting the proliferation of MDA-MB-231 cells, respectively, and inducing cell arrest at the G2/M phase may be the mechanism by which the compounds function in regulating the proliferation of MDA-MB-231 cells. Although the conformations of the preferred compounds were not determined, these findings provide a new direction for discovering small-molecule inhibitors with better antitumor activity and drug-forming properties than CTS.

Material and Methods

Reagents and Chemicals

Reagents (CTS, *N*-(chloroacetyl)glycine, *N*-chloroacetyl-DL-alanine, *N*-chloroacetyl-L-valine, *N*-chloroacetyl-DL-isoleucine, *N*-chloroacetyl-L-leucine, *N*-chloroacetyl-DL-phenylalanine, triphenylphosphine, and tricyclohexylphosphine, etc.) were obtained from Damas-Beta (Shanghai, China), Energy Chemical (Shanghai, China), and Tokyo Chemical Industry (Japan) and used directly without further purification. ^{1}H nuclear magnetic resonance (NMR) and ^{13}C NMR spectra were recorded on a Bruker DRX instrument (500 MHz for ^{1}H and 125 MHz for ^{13}C) that had been internally referenced to tetramethylsilane or chloroform-*d* ($CDCl_3$) signals (^{1}H: 7.26, ^{13}C: 77.16). The NMR samples were kept under vacuum before measurement to remove any possible solvate molecules. All reactions were monitored by thin-layer chromatography (TLC) using silica gel plates (silica gel 60 F254 0.25 mm).

MDA-MB-231 cells were obtained from the Cell Resource Center, Shanghai Institutes for Biological Sciences, Chinese Academy of Sciences. L-15 medium, penicillin-streptomycin solution, trypsin, dimethyl sulfoxide (DMSO), cell freezing medium, and Annexin V-FITC/PI cell apoptosis detection kit were acquired from Gibco (United States), Hyclone (United States), and CellMax (Beijing, China), Sinopharm Group (Shanghai, China), Beyotime (Shanghai, China), and Absin (Shanghai, China), respectively. Fetal bovine serum, cell cycle, and apoptosis detection kits were purchased from Yeasen (Shanghai, China). Sterile PBS, the CCK-8 kit, and the cell viability (dead cell staining) detection kit were all procured from Meilunbio (Dalian, China).

Synthesis of A1

To a solution of CTS (200 mg, 0.674 mmol) in chlorobenzene (6 mL) was added *N*-(chloroacetyl)glycine (204 mg,

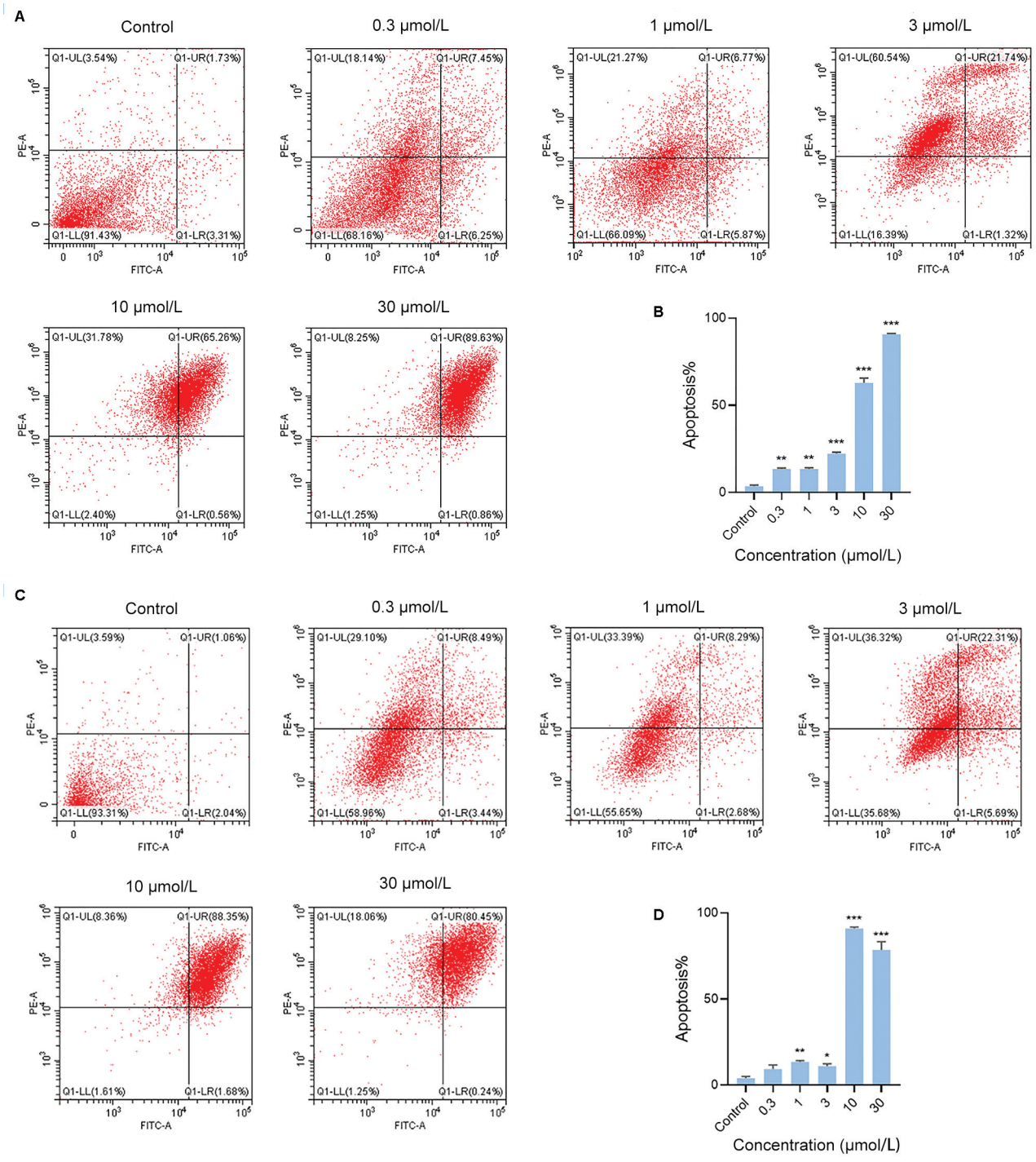

Fig. 3 (**A**) Flow cytometry demonstrated apoptosis of MDA-MB-231 cells exposed to different concentrations of **C4-2** for 12 hours and (**B**) the statistical results. (**C**) Flow cytometry demonstrated apoptosis of MDA-MB-231 cells exposed to different concentrations of **C5-2** for 12 hours and (**D**) the statistical results. $^{**}p \leq 0.01$, $^{***}p \leq 0.001$ versus the control.

1.349 mmol) and 2,2,6,6-tetramethylpiperidinooxy (TEMPO; 127 mg, 0.809 mmol). The reaction was stirred at 120°C for 24 hours and cooled to room temperature. Chlorobenzene was steamed. The residue was purified by silica gel column chromatography (petroleum ether/ethyl acetate [PE:EA] = 5–10%) to give **A1** (90 mg, 30%) as an orange-red solid. ^{1}H NMR (500 MHz, $CDCl_3$) δ 7.76 (d, J = 8.2 Hz, 1H), 7.70 (dd, J = 8.2, 1.3 Hz, 1H), 6.52 (d, J = 3.4 Hz, 1H), 5.00–4.86 (m, 1H), 4.40 (dd, J = 9.2, 5.7 Hz, 1H), 4.25–4.08 (m, 4H), 3.89–3.79 (m, 1H), 2.29–1.86 (m, 4H), 1.41 (d, J = 2.4 Hz, 3H), 1.36 (dd, J = 6.7, 2.8 Hz, 3H), 1.28 (d, J = 2.7 Hz, 3H). ^{13}C NMR (125 MHz, $CDCl_3$) δ 185.5, 179.2, 169.5, 167.88, 165.60, 153.34, 150.5, 132.96, 132.92, 126.79, 125.42, 107.8, 79.84, 76.78, 76.53, 68.49, 41.90, 40.96, 35.12, 31.42, 31.13, 30.50, 29.21, 22.20, 18.32. HRMS (ESI): m/z calcd. for $C_{23}H_{25}ClNO_6^+$ $[M+H]^+$ 446.1365, found 446.1367.

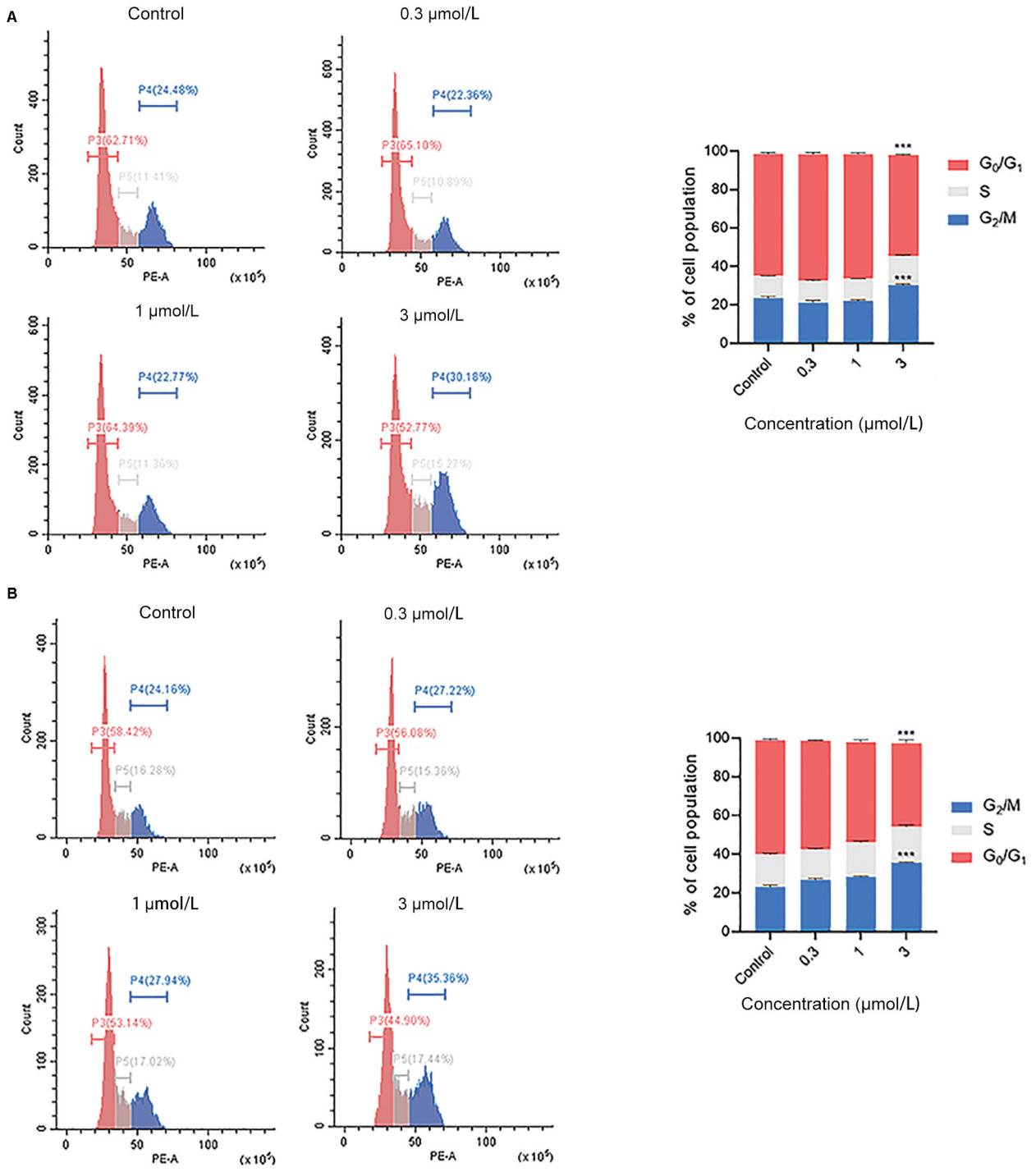

Fig. 4 Cell cycle distribution of MDA-MB-231 cells exposed to different concentrations of (**A**) **C4-2** and (**B**) **C5-2**. $^{***}p \leq 0.001$ versus control.

Synthesis of A2-1 and A2-2

Adopting the synthetic method of **A1** mentioned above, except the use of *N*-chloroacetyl-$_{DL}$-alanine (223 mg, 1.349 mmol) in place of *N*-(chloroacetyl)glycine, **A2-1** and its diastereoisomer **A2-2** were obtained.

A2-1, 110 mg, 32.3% yield, an orange-red solid. ^{1}H NMR (500 MHz, $CDCl_3$) δ 7.75 (d, J = 8.2 Hz, 1H), 7.69 (d, J = 8.2 Hz, 1H), 6.54 (dt, J = 15.4, 3.6 Hz, 1H), 4.91 (td, J = 9.5, 4.9 Hz, 1H), 4.52 (h, J = 6.9 Hz, 1H), 4.39 (ddd, J = 9.4, 6.0, 1.9 Hz, 1H), 4.08–3.99 (m, 2H), 3.69–3.53 (m, 1H), 2.29–1.81 (m, 4H), 1.42–1.23 (m, 12H). ^{13}C NMR (125 MHz, $CDCl_3$) δ 186.4, 178.9, 167.8, 166.88, 165.46, 152.31, 150.36, 133.52, 132.91, 129.07, 127.30, 108.92, 81.71, 77.06, 76.81, 68.55, 48.69, 42.51, 34.97, 32.08, 31.54, 31.22, 29.74, 24.57, 18.73, 18.42. HRMS (ESI): m/z calcd. for $C_{24}H_{27}ClNO_6^+$ $[M+H]^+$ 460.1521, found 460.1521.

A2-2, 142 mg, 41.8% yield, an orange solid. ^{1}H NMR (500 MHz, $CDCl_3$) δ 7.79–7.66 (m, 2H), 6.54 (dt, J = 15.4, 3.6 Hz, 1H), 4.91 (td, J = 9.5, 4.9 Hz, 1H), 4.57–4.35 (m, 2H), 4.03 (d, J = 22.7 Hz, 2H), 3.70–3.53 (m, 1H), 2.31–1.83 (m, 4H),

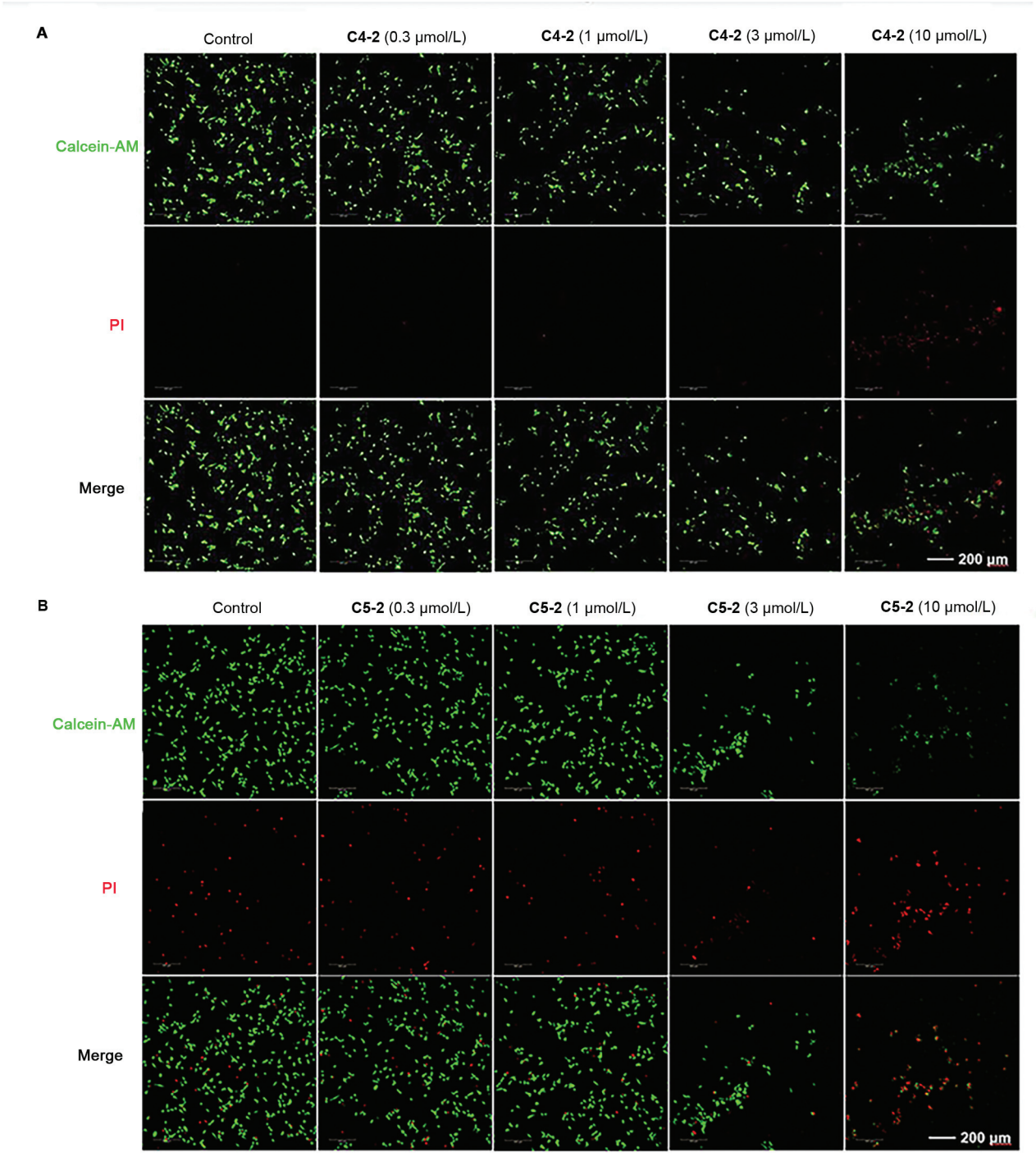

Fig. 5 The amount of live and dead cells when MDA-MB-231 cells were treated with different concentrations of (**A**) **C4-2** and (**B**) **C5-2**, revealed by Calcein-AM/PI staining.

Table 2 Water solubility of some derivatives

Compd.	Water solubility (μg/mL)
CTS	0.218
A4-2	24.513
A5-2	37.646
C4-2	172.585
C5-2	99.659

Note: $\lambda_{max} = 265$ nm.

1.41 (t, $J = 1.7$ Hz, 3H), 1.38–1.24 (m, 9H). ^{13}C NMR (125 MHz, $CDCl_3$) δ 187.6, 179.2, 168.8, 167.38, 166.49, 152.59, 150.48, 133.42, 132.18, 129.37, 126.79, 109.21, 81.71, 77.32, 77.06, 68.44, 48.69, 42.51, 32.08, 31.65, 31.54, 31.17, 29.74, 24.57, 18.88, 18.31. HRMS (ESI): *m/z* calcd. for $C_{24}H_{27}ClNO_6^+$ $[M+H]^+$ 460.1521, found 460.1523.

Synthesis of A3-1 and A3-2

Adopting the synthetic method of **A1** mentioned above, except the use of *N*-chloroacetyl-L-valine (261 mg, 1.349 mmol)

in place of *N*-(chloroacetyl)glycine, **A3-1** and its diastereoisomer **A3-2** were obtained.

A3-1, 62.1 mg, 18.9% yield, an orange-red solid. ^{1}H NMR (500 MHz, $CDCl_3$) δ 7.75 (d, J = 8.0 Hz, 1H), 7.69 (d, J = 8.1 Hz, 1H), 6.68 (s, 1H), 4.92 (t, J = 9.3 Hz, 1H), 4.58 (dd, J = 8.7, 4.6 Hz, 2H), 4.52–4.35 (m, 2H), 3.61 (s, 1H), 2.29 (pd, J = 7.0, 4.7 Hz, 2H), 1.95 (td, J = 26.9, 25.1, 14.4 Hz, 3H), 1.41 (s, 3H), 1.35 (d, J = 6.1 Hz, 3H), 1.26 (s, 3H), 0.99–0.80 (m, 6H). ^{13}C NMR (125 MHz, $CDCl_3$) δ 184.79, 176.43, 176.28, 171.86, 171.26, 167.78, 154.48, 137.70, 134.93, 128.58, 126.90, 120.12, 83.14, 78.70, 78.45, 78.19, 69.63, 59.05, 58.69, 43.97, 36.37, 36.10, 33.31, 32.97, 32.46, 25.79, 20.97, 20.36, 18.98. HRMS (ESI): *m/z* calcd. for $C_{26}H_{31}ClNO_6^+$ $[M+H]^+$ 488.1834, found 488.1831.

A3-2, 42.5 mg, 12.9% yield, an orange solid. ^{1}H NMR (500 MHz, $CDCl_3$) δ 7.75 (d, J = 8.2 Hz, 1H), 7.68 (d, J = 8.2 Hz, 1H), 6.61 (t, J = 3.3 Hz, 1H), 4.91 (t, J = 9.5 Hz, 1H), 4.57–4.36 (m, 2H), 4.15–4.06 (m, 2H), 3.61 (dp, J = 9.2, 6.6 Hz, 1H), 2.34–2.14 (m, 3H), 2.02–1.84 (m, 2H), 1.41 (s, 3H), 1.36 (d, J = 6.8 Hz, 3H), 1.28 (s, 3H), 1.01–0.90 (m, 6H). ^{13}C NMR (125 MHz, $CDCl_3$) δ 184.63, 176.34, 175.49, 171.63, 171.27, 167.42, 154.09, 137.53, 134.83, 128.68, 126.92, 120.18, 83.08, 78.69, 78.44, 78.18, 69.60, 58.76, 58.61, 44.12, 36.33, 36.08, 33.10, 32.87, 32.59, 25.91, 20.39, 20.10, 18.98. HRMS (ESI): *m/z* calcd. for $C_{26}H_{31}ClNO_6^+$ $[M+H]^+$ 488.1834, found 488.1834.

Synthesis of A4-1 and A4-2

Adopting the synthetic method of **A1** mentioned above, except the use of *N*-chloroacetyl-DL-isoleucine (280 mg, 1.349 mmol) in place of *N*-(chloroacetyl)glycine, **A4-1** and its diastereoisomer **A4-2** were obtained.

A4-1, 90 mg, 26.6% yield, an orange-red solid. ^{1}H NMR (500 MHz, $CDCl_3$) δ 7.74 (dd, J = 8.2, 2.5 Hz, 1H), 7.68 (d, J = 8.1 Hz, 1H), 6.71–6.59 (m, 1H), 4.90 (td, J = 9.6, 4.1 Hz, 1H), 4.58 (ddd, J = 20.1, 9.0, 4.0 Hz, 1H), 4.38 (dd, J = 9.3, 6.1 Hz, 1H), 4.18–3.98 (m, 2H), 3.61 (ddt, J = 12.7, 9.1, 6.4 Hz, 1H), 2.31–1.74 (m, 4H), 1.64–1.52 (m, 1H), 1.51–1.43 (m, 1H), 1.41 (s, 3H), 1.36 (dd, J = 11.3, 7.0 Hz, 3H), 1.27 (s, 3H), 1.16 (dp, J = 14.7, 7.6 Hz, 1H), 1.04–0.77 (m, 6H). ^{13}C NMR (125 MHz, $CDCl_3$) δ 183.44, 175.02, 174.89, 170.08, 165.94, 136.37, 136.25, 129.06, 127.30, 127.26, 125.43, 118.68, 81.61, 77.31, 77.06, 76.80, 68.25, 56.02, 42.77, 37.45, 34.99, 34.94, 34.74, 31.99, 31.65, 31.25, 24.43, 18.74, 14.01, 11.69. HRMS (ESI): *m/z* calcd. for $C_{27}H_{33}ClNO_6^+$ $[M+H]^+$ 502.1991, found 502.1992.

A4-2, 96 mg, 28.4% yield, an orange-red solid. ^{1}H NMR (500 MHz, $CDCl_3$) δ 7.76–7.65 (m, 2H), 6.61 (t, J = 3.4 Hz, 1H), 4.90 (t, J = 9.5 Hz, 1H), 4.56–4.32 (m, 2H), 4.18–3.98 (m, 2H), 3.60 (dp, J = 9.6, 6.7 Hz, 1H), 2.31–1.83 (m, 4H), 1.65–1.55 (m, 1H), 1.45–1.20 (m, 11H), 0.96–0.83 (m, 6H). ^{13}C NMR (125 MHz, $CDCl_3$) δ 183.20, 174.90, 170.12, 169.94, 165.71, 152.64, 136.15, 133.43, 128.89, 127.32, 125.51, 118.80, 81.65, 77.31, 77.06, 76.80, 68.19, 56.82, 42.74, 38.02, 34.92, 34.71, 32.10, 31.72, 31.19, 24.97, 24.52, 18.71, 15.34, 11.58. HRMS (ESI): *m/z* calcd. for $C_{27}H_{33}ClNO_6^+$ $[M+H]^+$ 502.1991, found 502.1993.

Synthesis of A5-1 and A5-2

Adopting the synthetic method of **A1** mentioned above, except the use of *N*-chloroacetyl-L-leucine (280 mg, 1.349 mmol) in place of *N*-(chloroacetyl)glycine, **A5-1** and its diastereoisomer **A5-2** were obtained.

A5-1, 60 mg, 17.7% yield, an orange-red solid. ^{1}H NMR (500 MHz, $CDCl_3$) δ 7.75 (d, J = 8.2 Hz, 1H), 7.69 (d, J = 8.2 Hz, 1H), 6.57 (d, J = 3.9 Hz, 1H), 4.91 (t, J = 9.5 Hz, 1H), 4.56 (ddd, J = 10.2, 8.7, 4.6 Hz, 1H), 4.39 (dd, J = 9.3, 6.0 Hz, 1H), 4.07 (d, J = 5.4 Hz, 2H), 3.67–3.56 (m, 1H), 2.26–2.14 (m, 2H), 2.03–1.89 (m, 2H), 1.64–1.48 (m, 3H), 1.42 (s, 3H), 1.36 (d, J = 6.8 Hz, 3H), 1.27 (d, J = 5.4 Hz, 3H), 0.86 (d, J = 6.4 Hz, 3H), 0.84 (d, J = 6.4 Hz, 3H). ^{13}C NMR (125 MHz, $CDCl_3$) δ 184.95, 176.35, 172.32, 171.54, 167.27, 154.38, 137.83, 134.85, 130.46, 128.62, 126.79, 120.09, 83.04, 78.68, 78.43, 78.18, 69.69, 52.69, 43.97, 42.52, 36.36, 36.10, 33.40, 32.94, 32.63, 26.27, 25.88, 24.46, 22.91, 20.28. HRMS (ESI): *m/z* calcd. for $C_{27}H_{33}ClNO_6^+$ $[M+H]^+$ 502.1991, found 502.1991.

A5-2, 60 mg, 17.7% yield, an orange-red solid. ^{1}H NMR (500 MHz, $CDCl_3$) δ 7.75 (d, J = 8.2 Hz, 1H), 7.69 (d, J = 8.2 Hz, 1H), 6.57 (d, J = 3.8 Hz, 1H), 4.91 (t, J = 9.5 Hz, 1H), 4.56 (ddd, J = 10.2, 8.7, 4.6 Hz, 1H), 4.39 (dd, J = 9.3, 6.0 Hz, 1H), 4.07 (d, J = 5.4 Hz, 2H), 3.68–3.55 (m, 1H), 2.26–2.16 (m, 2H), 2.02–1.89 (m, 2H), 1.64–1.49 (m, 3H), 1.42 (s, 3H), 1.36 (d, J = 6.8 Hz, 3H), 1.27 (s, 3H), 0.86 (d, J = 6.4 Hz, 3H), 0.84 (d, J = 6.4 Hz, 3H). ^{13}C NMR (125 MHz, $CDCl_3$) δ 184.95, 176.35, 172.32, 171.54, 167.27, 154.38, 137.83, 134.85, 130.46, 128.62, 126.79, 120.09, 83.04, 78.68, 78.43, 78.18, 69.69, 52.69, 43.97, 42.52, 36.36, 36.10, 33.40, 32.94, 32.63, 26.27, 25.88, 24.46, 22.91, 20.28. HRMS (ESI): *m/z* calcd. for $C_{27}H_{33}ClNO_6^+$ $[M+H]^+$ 502.1991, found 502.1991.

Synthesis of A6-1 and A6-2

Adopting the synthetic method of **A1** mentioned above, except the use of *N*-chloroacetyl-DL-phenylalanine (326 mg, 1.349 mmol) in place of *N*-(chloroacetyl)glycine, **A6-1** and its diastereoisomer **A6-2** were obtained.

A6-1, 44 mg, 12.2% yield, an orange-red solid. ^{1}H NMR (500 MHz, $CDCl_3$) δ 7.76–7.65 (m, 2H), 7.27–7.22 (m, 1H), 7.20–7.13 (m, 3H), 7.02 (dd, J = 39.9, 7.9 Hz, 1H), 6.53 (dt, J = 13.7, 3.4 Hz, 1H), 4.95–4.70 (m, 2H), 4.38 (ddd, J = 9.3, 6.1, 3.1 Hz, 1H), 4.10–3.79 (m, 2H), 3.60 (tdd, J = 9.6, 7.5, 4.5 Hz, 1H), 3.34–2.95 (m, 2H), 2.29–1.43 (m, 4H), 1.40–1.32 (m, 6H), 1.25 (d, J = 5.7 Hz, 3H). ^{13}C NMR (125 MHz, $CDCl_3$) δ 183.60, 175.07, 170.25, 169.83, 165.64, 152.97, 136.16, 133.59, 129.37, 129.26, 128.46, 128.34, 127.20, 126.99, 126.81, 125.48, 118.77, 118.69, 81.68, 77.34, 77.08, 76.83, 68.68, 53.53, 42.52, 37.99, 34.88, 34.71, 31.89, 31.67, 31.15, 24.51, 18.90. HRMS (ESI): *m/z* calcd. for $C_{30}H_{31}ClNO_7^+$ $[M+H]^+$ 536.1834, found 536.1837.

A6-2, 107 mg, 29.6% yield, an orange-red solid. ^{1}H NMR (500 MHz, $CDCl_3$) δ 7.76–7.65 (m, 2H), 7.27–7.22 (m, 1H), 7.20–7.13 (m, 3H), 7.02 (dd, J = 39.9, 7.9 Hz, 1H), 6.53 (dt, J = 13.7, 3.4 Hz, 1H), 4.95–4.70 (m, 2H), 4.38 (ddd, J = 9.3, 6.1, 3.1 Hz, 1H), 4.10–3.79 (m, 2H), 3.60 (tdd, J = 9.6, 7.5, 4.5 Hz, 1H), 3.34–2.95 (m, 2H), 2.29–1.43 (m, 4H), 1.40–1.32 (m, 6H), 1.25 (d, J = 5.7 Hz, 3H). ^{13}C NMR (125 MHz, $CDCl_3$) δ 183.60, 175.07, 170.25, 169.83, 165.64, 152.97, 136.16, 133.59,

129.37, 129.26, 128.46, 128.34, 127.20, 126.99, 126.81, 125.48, 118.77, 118.69, 81.68, 77.34, 77.08, 76.83, 68.68, 53.53, 42.52, 37.99, 34.88, 34.71, 31.89, 31.67, 31.15, 24.51, 18.90. HRMS (ESI): *m/z* calcd. for $C_{30}H_{31}ClNO_6^+$ $[M+H]^+$ 536.1834, found 536.1837.

Synthesis of B1

To a solution of **A1** (50 mg, 0.112 mmol) in acetonitrile (6 mL) was added triphenylphosphine (58.9 mg, 0.224 mmol). The reaction mixture was refluxed at 80°C for 4 hours. After the completion of the reaction monitored by TLC, the reaction mixture was cooled to room temperature. The acetonitrile was steamed. The residue was purified by silica gel column chromatography (dichloromethane:methanol = 5–10%) to obtain **B1** (15 mg, 18.9%) as an orange solid. ^{1}H NMR (500 MHz, $CDCl_3$) δ 7.76 (d, J = 8.2 Hz, 1H), 7.67–7.65 (m, 7H), 7.55–7.51 (m, 7H), 7.44 (d, J = 2.7 Hz, 2H), 6.52 (q, J = 3.1 Hz, 1H), 4.91 (td, J = 9.5, 3.2 Hz, 1H), 4.39 (dd, J = 9.4, 6.0 Hz, 1H), 4.29–3.98 (m, 3H), 3.84 (ddd, J = 18.3, 10.0, 3.7 Hz, 1H), 3.61 (ddd, J = 10.3, 8.5, 5.2 Hz, 1H), 2.29–1.84 (m, 4H), 1.40 (d, J = 2.3 Hz, 3H), 1.36 (dd, J = 6.8, 2.6 Hz, 3H), 1.28 (s, 3H). HRMS (ESI): *m/z* calcd. for $C_{41}H_{39}NO_6P^+$ $[M]^+$ 672.2515 found 672.2513.

Synthesis of B2-1

Adopting the synthetic method of **B1** mentioned above, **A2-1** (50 mg, 0.109 mmol) was used as the starting material to obtain **B2-1** (20 mg, 25.8%) as an orange solid. ^{1}H NMR (500 MHz, $CDCl_3$) δ 7.87–7.81 (m, 6H), 7.78–7.71 (m, 3H), 7.64 (dddd, J = 13.1, 6.9, 5.5, 3.7 Hz, 8H), 6.51–6.42 (m, 1H), 5.33–5.15 (m, 1H), 5.11–4.82 (m, 2H), 4.47–4.28 (m, 1H), 4.17–4.04 (m, 1H), 3.70–3.44 (m, 1H), 2.27–2.08 (m, 2H), 2.00–1.83 (m, 2H), 1.36 (d, J = 2.9 Hz, 3H), 1.34–1.21 (m, 9H). HRMS (ESI): *m/z* calcd. for $C_{42}H_{41}NO_6P^+$ $[M]^+$ 686.2671, found 686.2671.

Synthesis of B2-2

Adopting the synthetic method of **B1** mentioned above, **A2-2** (50 mg, 0.109 mmol) was used as the starting material to obtain **B2-2** (7.4 mg, 9.7%) as an orange solid. ^{1}H NMR (500 MHz, $CDCl_3$) δ 7.89–7.80 (m, 6H), 7.77–7.71 (m, 3H), 7.63 (ddd, J = 8.1, 3.5, 1.6 Hz, 5H), 7.58–7.43 (m, 3H), 6.56–6.39 (m, 1H), 5.37–5.17 (m, 1H), 5.11–4.80 (m, 2H), 4.45–4.29 (m, 1H), 4.21–4.05 (m, 1H), 3.66–3.43 (m, 1H), 2.20–1.85 (m, 4H), 1.38–1.34 (m, 3H), 1.32–1.21 (m, 9H). HRMS (ESI): *m/z* calcd. for $C_{42}H_{41}NO_6P^+$ $[M]^+$ 686.2671, found 686.2671.

Synthesis of B3-1

Adopting the synthetic method of **B1** mentioned above, **A3-1** (50 mg, 0.103 mmol) was used as the starting material to obtain **B3-1** (5 mg, 6.5%) as an orange solid. ^{1}H NMR (500 MHz, $CDCl_3$) δ 7.91–7.84 (m, 6H), 7.73 (dd, J = 7.7, 1.8 Hz, 4H), 7.66–7.60 (m, 7H), 6.63–6.58 (m, 1H), 5.51 (dd, J = 16.3, 12.8 Hz, 1H), 5.15–4.85 (m, 2H), 4.31 (dd, J = 9.2, 6.4 Hz, 1H), 4.02 (dt, J = 16.1, 8.1 Hz, 1H), 3.65–3.56 (m, 1H), 2.17 (s, 1H), 2.05–1.83 (m, 4H), 1.38 (d, J = 2.9 Hz, 3H), 1.25 (s, 6H), 0.88–0.80 (m, 6H). HRMS (ESI): *m/z* calcd. for $C_{44}H_{45}NO_6P^+$ $[M]^+$ 714.2984, found 714.2987.

Synthesis of B3-2

Adopting the synthetic method of **B1** mentioned above, **A3-2** (50 mg, 0.103 mmol) was used as the starting material to obtain **B3-2** (6 mg, 7.9%) as an orange solid. ^{1}H NMR (500 MHz, $CDCl_3$) δ 7.85 (dd, J = 13.2, 7.8 Hz, 7H), 7.77–7.71 (m, 2H), 7.69–7.64 (m, 8H), 6.60 (d, J = 3.5 Hz, 1H), 5.60 (t, J = 14.7 Hz, 1H), 5.19–4.83 (m, 2H), 4.43–4.29 (m, 1H), 4.15 (dd, J = 7.7, 4.9 Hz, 1H), 3.68–3.53 (m, 1H), 2.63 (s, 1H), 2.17 (s, 4H), 1.38–1.33 (m, 6H), 1.34–1.26 (m, 3H), 0.97 (dd, J = 10.4, 6.8 Hz, 3H), 0.86 (s, 3H). HRMS (ESI): *m/z* calcd. for $C_{44}H_{45}NO_6P^+$ $[M]^+$ 714.2984, found 714.2984.

Synthesis of B4-1

Adopting the synthetic method of **B1** mentioned above, **A4-1** (50 mg, 0.099 mmol) was used as the starting material to obtain **B4-1** (12 mg, 15.7%) as an orange solid. ^{1}H NMR (500 MHz, $CDCl_3$) δ 7.89–7.82 (m, 7H), 7.67–7.60 (m, 8H), 7.50 (ddd, J = 35.6, 7.7, 2.4 Hz, 2H), 6.56 (t, J = 3.8 Hz, 1H), 5.16–4.96 (m, 1H), 4.86 (t, J = 9.6 Hz, 1H), 4.43–4.25 (m, 2H), 4.16 (q, J = 6.8, 5.7 Hz, 1H), 3.68–3.53 (m, 1H), 2.24–2.15 (m, 2H), 2.04–1.81 (m, 3H), 1.38 (s, 5H), 1.34–1.25 (m, 6H), 0.84 (d, J = 6.8 Hz, 3H), 0.80–0.71 (m, 3H). HRMS (ESI): *m/z* calcd. for $C_{45}H_{47}NO_6P^+$ $[M]^+$ 728.3141, found 728.3145.

Synthesis of B5-1

Adopting the synthetic method of **B1** mentioned above, **A5-1** (50 mg, 0.099 mmol) was used as the starting material to obtain **B5-1** (20 mg, 26.3%) as an orange solid. ^{1}H NMR (600 MHz, methanol-d_4) δ 7.75 (dd, J = 13.6, 6.5 Hz, 8H), 7.64–7.62 (m, 6H), 7.55 (t, J = 9.7 Hz, 2H), 7.46 (s, 1H), 5.39 (s, 1H), 4.91 (t, J = 9.6 Hz, 1H), 4.39–4.33 (m, 1H), 4.21–4.12 (m, 2H), 3.56 (s, 1H), 2.08 (d, J = 6.0 Hz, 2H), 1.94 (dt, J = 28.5, 13.9 Hz, 4H), 1.79 (d, J = 20.7 Hz, 3H), 1.29 (s, 3H), 1.22–1.19 (m, 6H), 0.69 (d, J = 5.9 Hz, 3H), 0.58 (d, J = 5.7 Hz, 3H). HRMS (ESI): *m/z* calcd. for $C_{45}H_{47}NO_6P^+$ $[M]^+$ 728.3141, found 728.3143.

Synthesis of B6-1

Adopting the synthetic method of **B1** mentioned above, **A6-1** (50 mg, 0.093 mmol) was used as the starting material to obtain **B6-1** (23 mg, 13.3%) as an orange solid. HRMS (ESI): *m/z* calcd. for $C_{48}H_{45}NO_6P^+$ $[M]^+$ 762.2984, found 762.2987.

Synthesis of C1

To a solution of **A1** (50 mg, 0.112 mmol) in acetonitrile (6 mL) was added tricyclohexylphosphine (63 mg, 0.224 mmol). The reaction mixture was refluxed at 80°C for 40 minutes, and cooled to room temperature. The acetonitrile was steamed. The residue was purified by silica gel column chromatography (DCM:MeOH = 5–10%) to give **C1** (24 mg, 29.6%) as an orange solid. ^{1}H NMR (500 MHz, $CDCl_3$) δ 7.71 (d, J = 8.2 Hz, 1H), 7.64 (d, J = 8.3 Hz, 1H), 6.52 (dq, J = 7.4, 3.8 Hz, 1H), 4.88 (t, J = 9.5 Hz, 1H), 4.35 (ddd, J = 9.5, 6.1, 3.5 Hz, 1H), 4.15–3.98 (m, 2H), 3.85–3.52 (m, 3H), 2.64–2.55 (m, 3H), 2.40 (s, 3H), 2.24–1.48 (m, 31H), 1.39 (d, J = 2.4 Hz, 3H), 1.34–1.21 (m, 6H). HRMS (ESI): *m/z* calcd. for $C_{41}H_{57}NO_6P^+$ $[M]^+$ 690.3924, found 690.3926.

Synthesis of C2-1

Adopting the synthetic method of **C1** mentioned above, **A2-1** (50 mg, 0.108 mmol) was used as the starting material to obtain **C2-1** (25 mg, 31.2%) as an orange solid. ^{1}H NMR (500 MHz, $CDCl_3$) δ 7.72–7.69 (m, 1H), 7.65 (dd, J = 8.2, 2.0 Hz, 1H), 6.52–6.44 (m, 1H), 4.89 (td, J = 9.5, 4.8 Hz, 1H), 4.39–4.14 (m, 3H), 3.64–3.55 (m, 2H), 2.63–2.55 (m, 4H), 2.08–1.89 (m, 21H), 1.78 (d, J = 9.3 Hz, 4H), 1.61 (d, J = 9.3 Hz, 8H), 1.41–1.38 (m, 6H), 1.34 (d, J = 3.7 Hz, 3H), 1.25 (d, J = 2.3 Hz, 3H). HRMS (ESI): *m/z* calcd. for $C_{42}H_{59}NO_6P^+$ $[M]^+$ 704.4080, found 704.4082.

Synthesis of C2-2

Adopting the synthetic method of **C1** mentioned above, **A2-2** (50 mg, 0.108 mmol) was used as the starting material to obtain **C2-2** (20 mg, 25.0%) as an orange solid. ^{1}H NMR (500 MHz, $CDCl_3$) δ 7.71 (d, J = 5.4 Hz, 1H), 7.65 (d, J = 8.2 Hz, 1H), 6.70–6.63 (m, 1H), 4.88 (t, J = 9.5 Hz, 1H), 4.37–4.13 (m, 3H), 3.69–3.53 (m, 2H), 2.70–2.56 (m, 4H), 2.07 (s, 8H), 1.93 (s, 13H), 1.77 (d, J = 10.4 Hz, 4H), 1.65–1.58 (m, 8H), 1.52–1.47 (m, 6H), 1.34 (d, J = 6.7 Hz, 3H), 1.25 (s, 3H). HRMS (ESI): *m/z* calcd. for $C_{42}H_{59}NO_6P^+$ $[M]^+$ 704.4080, found 704.4083.

Synthesis of C3-1

Adopting the synthetic method of **C1** mentioned above, **A3-1** (50 mg, 0.102 mmol) was used as the starting material to obtain **C3-1** (12 mg, 15.2%) as an orange solid. ^{1}H NMR (500 MHz, $CDCl_3$) δ 7.68 (d, J = 8.2 Hz, 1H), 7.63 (d, J = 8.2 Hz, 1H), 6.61 (s, 1H), 4.97 (t, J = 9.4 Hz, 1H), 4.31 (dd, J = 9.0, 6.2 Hz, 1H), 4.12–4.04 (m, 2H), 3.99–3.90 (m, 1H), 3.67–3.59 (m, 1H), 2.70–2.61 (m, 4H), 2.12–1.89 (m, 20H), 1.79–1.57 (m, 14H), 1.38–1.31 (m, 9H), 1.01 (d, J = 6.6 Hz, 3H), 0.97 (d, J = 6.7 Hz, 3H). HRMS (ESI): *m/z* calcd. for $C_{44}H_{63}NO_6P^+$ $[M]^+$ 732.4393, found 732.4396.

Synthesis of C3-2

Adopting the synthetic method of **C1** mentioned above, **A3-2** (50 mg, 0.102 mmol) was used as the starting material to obtain **C3-2** (5 mg, 16.3%) as an orange solid. ^{1}H NMR (500 MHz, $CDCl_3$) δ 7.71 (d, J = 8.2 Hz, 1H), 7.65 (d, J = 8.2 Hz, 1H), 6.71 (s, 1H), 4.88 (t, J = 9.5 Hz, 1H), 4.52 (s, 1H), 4.35 (dd, J = 9.3, 6.4 Hz, 1H), 4.10 (s, 1H), 3.66–3.54 (m, 2H), 2.77–2.63 (m, 4H), 2.13 (s, 6H), 1.99–1.87 (m, 14H), 1.76 (d, J = 10.8 Hz, 4H), 1.63 (d, J = 12.5 Hz, 6H), 1.52 (d, J = 9.8 Hz, 4H), 1.38–1.33 (m, 9H), 1.13 (d, J = 6.5 Hz, 3H), 1.03 (d, J = 6.7 Hz, 3H). HRMS (ESI): *m/z* calcd. for $C_{44}H_{63}NO_6P^+$ $[M]^+$ 732.4393, found 732.4394.

Synthesis of C4-1

Adopting the synthetic method of **C1** mentioned above, **A4-1** (90 mg, 0.179 mmol) was used as the starting material to obtain **C4-1** (60 mg, 37.5%) as an orange solid. ^{1}H NMR (500 MHz, $CDCl_3$) δ 7.68 (d, J = 8.4 Hz, 1H), 7.64 (d, J = 3.6 Hz, 1H), 6.78–6.65 (m, 1H), 4.86 (t, J = 9.5 Hz, 1H), 4.38–4.32 (m, 1H), 4.24–4.10 (m, 1H), 3.77–3.48 (m, 2H), 2.68–2.55 (m, 4H), 2.07 (d, J = 10.0 Hz, 4H), 1.97–1.46 (m, 33H), 1.23 (d, J = 4.1 Hz, 9H), 1.10–1.07 (m, 3H), 0.84 (d, J = 6.8 Hz, 3H). HRMS (ESI): *m/z* calcd. for $C_{45}H_{65}NO_6P^+$ $[M]^+$ 746.4550, found 745.4556.

Synthesis of C4-2

Adopting the synthetic method of **C1** mentioned above, **A4-2** (90 mg, 0.179 mmol) was used as the starting material to obtain **C4-2** (24 mg, 15.4%) as an orange solid. ^{1}H NMR (500 MHz, $CDCl_3$) δ 7.71 (d, J = 8.2 Hz, 1H), 7.65 (d, J = 8.2 Hz, 1H), 6.75–6.66 (m, 1H), 4.88 (t, J = 9.5 Hz, 1H), 4.41–4.30 (m, 1H), 4.26–4.13 (m, 1H), 3.69–3.51 (m, 2H), 2.75–2.59 (m, 4H), 2.24–2.10 (m, 7H), 2.04–1.47 (m, 30H), 1.39–1.23 (m, 9H), 1.01 (dd, J = 7.0, 3.9 Hz, 3H), 0.87 (t, J = 7.3 Hz, 3H). HRMS (ESI): *m/z* calcd. for $C_{45}H_{65}NO_6P^+$ $[M]^+$ 746.4550, found 745.4552.

Synthesis of C5-1

Adopting the synthetic method of **C1** mentioned above, **A5-1** (50 mg, 0.099 mmol) was used as the starting material to obtain **C5-1** (28 mg, 35.9%) as an orange solid. ^{1}H NMR (500 MHz, $CDCl_3$) δ 7.70–7.61 (m, 2H), 6.52 (dt, J = 20.4, 3.5 Hz, 1H), 4.91 (t, J = 9.5 Hz, 1H), 4.42–4.30 (m, 1H), 3.99 (dddd, J = 94.0, 16.1, 12.7, 3.8 Hz, 2H), 3.71–3.53 (m, 1H), 2.60 (ddd, J = 13.0, 10.4, 3.1 Hz, 4H), 2.23–1.51 (m, 37H), 1.40–1.22 (m, 9H), 0.87 (dq, J = 7.0, 3.4 Hz, 3H), 0.81 (d, J = 6.0 Hz, 3H). HRMS (ESI): *m/z* calcd. for $C_{45}H_{65}NO_6P^+$ $[M]^+$ 746.4550, found 745.4550.

Synthesis of C5-2

Adopting the synthetic method of **C1** mentioned above, **A5-2** (50 mg, 0.099 mmol) was used as the starting material to obtain **C5-2** (30 mg, 38.4%) as an orange solid. ^{1}H NMR (500 MHz, $CDCl_3$) δ 7.72–7.60 (m, 2H), 6.78–6.65 (m, 1H), 4.86 (t, J = 9.5 Hz, 1H), 4.40–4.19 (m, 2H), 3.73–3.50 (m, 2H), 2.74–2.55 (m, 4H), 2.17–1.50 (m, 37H), 1.36 (s, 3H), 1.33–1.30 (m, 3H), 1.23 (s, 3H), 0.91 (dd, J = 6.3, 2.9 Hz, 3H), 0.83 (dd, J = 6.3, 3.0 Hz, 3H). HRMS (ESI): *m/z* calcd. for $C_{45}H_{65}NO_6P^+$ $[M]^+$: 746.4550 found 745.4552.

Synthesis of C6-1

Adopting the synthetic method of **C1** mentioned above, **A6-1** (50 mg, 0.093 mmol) was used as the starting material to obtain **C6-1** (13 mg, 17.1%) as an orange solid. ^{1}H NMR (500 MHz, $CDCl_3$) δ 7.61 (d, J = 7.1 Hz, 2H), 7.18–7.11 (m, 5H), 6.72 (s, 1H), 4.86 (t, J = 9.5 Hz, 1H), 4.40 (q, J = 7.1 Hz, 1H), 4.33 (dd, J = 9.4, 6.1 Hz, 1H), 4.24 (d, J = 13.0 Hz, 1H), 3.52–3.43 (m, 2H), 3.26–3.12 (m, 4H), 2.75–2.68 (m, 4H), 1.92 (s, 8H), 1.84 (s, 7H), 1.72 (s, 6H), 1.58–1.55 (m, 10H), 1.33 (d, J = 6.6 Hz, 6H), 1.14 (s, 3H). HRMS (ESI): *m/z* calcd. for $C_{48}H_{63}NO_6P^+$ $[M]^+$ 780.4393, found 780.4395.

Synthesis of C6-2

Adopting the synthetic method of **C1** mentioned above, **A6-2** (50 mg, 0.093 mmol) was used as the starting material to obtain **C6-2** (23 mg, 32.6%) as an orange solid. ^{1}H NMR (600 MHz, methanol-d_4) δ 7.79 (d, J = 8.3 Hz, 1H), 7.66 (d, J = 8.2 Hz, 1H), 7.19–7.10 (m, 5H), 5.39 (s, 1H), 4.90 (t, J = 9.6 Hz, 1H), 4.53 (t, J = 7.7 Hz, 1H), 4.36 (dd, J = 9.4, 6.5 Hz, 1H), 3.66 (t, J = 6.7 Hz, 1H), 3.03 (d, J = 7.7 Hz, 1H), 2.90 (dd, J = 13.8, 7.6 Hz, 1H), 2.66–2.56 (m, 3H), 2.47 (d, J = 8.1 Hz, 1H), 2.30 (t, J = 6.7 Hz, 1H), 2.07 (q, J = 7.6 Hz, 2H), 2.02 (s, 1H), 1.92 (d, J = 10.3 Hz, 3H), 1.80 (s, 5H), 1.71–1.64

(m, 5H), 1.50–1.44 (m, 4H), 1.40–1.35 (m, 3H), 1.30–1.15 (m, 20H). HRMS (ESI): *m/z* calcd. for $C_{48}H_{63}NO_6P^+$ $[M]^+$ 780.4393, found 780.4391.

CCK-8 Assay

MDA-MB-231 cells were incubated in an L-15 complete medium at 37°C in a closed T25 incubator. Cells, in the logarithmic growth phase, were collected and inoculated in a 96-well plate at 1.2×10^5 cells/100 µL/well. Next, a solution of a derivative of CTS in a basal medium (L-15) was added for cell treatment. The experiment included a control group (cells were only treated with a medium of L-15) and three treatment groups (cells were treated with 0.3, 3, and 30 µmol/L of a derivative of CTS in a medium of L-15). Each group has five replicate wells in which the content of DMSO was less than 0.5%. After treatment of 24 hours, the medium was discarded, and then L-15 medium (100 µL) containing CCK-8 (v/v, 10%) was added under light protection. After 3 hours of incubation. The absorbance (OD) of each well was detected at 450 nm using a multifunctional enzyme labeling instrument (Spark, from Tecan, Switzerland).

Detection of Apoptosis Using Flow Cytometry

Cells were treated with different concentrations of 0.3, 3, and 30 µmol/L of **C4-2** and **C5-2**, and the cell cycle was measured using the Operetta CLS system after staining with PI/RNase staining buffer. Cells were stained with an Annexin V-FITC/PI apoptosis detection kit according to the manufacturer's instructions. The percentage of apoptotic cells was analyzed using a flow cytometry assay with Annexin V^+/PI^+ being seen in the upper right quadrant.

Calcein-AM/PI Staining of Live and Dead Cells

The medium was discarded from cells cultured in a 96-well plate. After washing the cells with PBS two to three times, an appropriate volume of Calcein-AM/PI working solution was added. Cells were incubated in the dark at 37°C for 15 to 30 minutes. After incubation, the intensity of staining was observed under a fluorescence microscope (Calcein-AM exhibiting green fluorescence, and PI exhibiting red fluorescence). Dead cells are characterized by a strong fluorescence signal at 645 nm and a weak fluorescence signal at 530 nm. The percentage of live and dead cells was calculated from the fluorescence readings as follows:

$$\text{Live cells\%} = (F(530)\text{sam} - F(530)\text{min})/(F(530)\text{max} - F(530)\text{min})$$

$$\text{Dead cells\%} = (F(645)\text{sam} - F(645)\text{min})/(F(645)\text{max} - F(645)\text{min})$$

where sam is the sample, max is the maximum, and min is the minimum.

Water Solubility Determination

Excess amounts of the test compounds were dissolved in PBS (200 µL), sonicated, allowed to stand at room temperature for 24 hours, and filtered through a 0.45-µmol/L microporous filter membrane. The filtrate (100 µL) was diluted to 1.5 mL with PBS, 10 µL of which was injected into the sample for high-performance liquid chromatography analysis. The peak area was recorded. The water solubility of the compound was calculated using a standard curve equation.

Data Analysis

Data are expressed as the mean ± standard deviation of at least three parallels. GraphPad Prism 8 software was used for analysis. Differences between groups were analyzed using a *t*-test or two-factor analysis of variance with a *p*-value ≤ 0.05 being statistical significance.

Supporting Information

Spectroscopic characterization processes (^{1}H NMR and ^{13}C NMR) for compounds **A1** to **A6-2**, **B1** to **B5-1**, and **C1** to **C6-2** are included in the Supporting Information (►**Supplementary Figs. S1–S29** [available in the online version]).

Funding

This work was supported by the National Key Laboratory of Lead Druggability Research (Grant No. NKLYT2023010) and the Three-year Action Plan for Shanghai TCM Development and Inheritance Program (Grant No. ZY [2021-2023]-0401).

Conflict of Interest

None declared.

References

1 Michaels E, Worthington RO, Rusiecki J. Breast cancer: risk assessment, screening, and primary prevention. Med Clin North Am 2023;107(02):271–284
2 Singh DD, Yadav DK. TNBC: potential targeting of multiple receptors for a therapeutic breakthrough, nanomedicine, and immunotherapy. Biomedicines 2021;9(08):876
3 Ferrari P, Scatena C, Ghilli M, Bargagna I, Lorenzini G, Nicolini A. Molecular mechanisms, biomarkers and emerging therapies for chemotherapy-resistant TNBC. Int J Mol Sci 2022;23(03):1665
4 Deng LJ, Qi M, Li N, Lei YH, Zhang DM, Chen JX. Natural products and their derivatives: promising modulators of tumor immunotherapy. J Leukoc Biol 2020;108(02):493–508
5 Li H, Gao C, Liu C, et al. A review of the biological activity and pharmacology of cryptotanshinone, an important active constituent in Danshen. Biomed Pharmacother 2021;137:111332
6 Pan Y, Shi J, Ni W, et al. Cryptotanshinone inhibition of mammalian target of rapamycin pathway is dependent on oestrogen receptor alpha in breast cancer. J Cell Mol Med 2017;21(09):2129–2139
7 Zhou J, Xu XZ, Hu YR, Hu AR, Zhu CL, Gao GS. Cryptotanshinone induces inhibition of breast tumor growth by cytotoxic CD4+ T cells through the JAK2/STAT4/ perforin pathway. Asian Pac J Cancer Prev 2014;15(06):2439–2445
8 Park IJ, Kim MJ, Park OJ, et al. Cryptotanshinone induces ER stress-mediated apoptosis in HepG2 and MCF7 cells. Apoptosis 2012;17 (03):248–257
9 Kobryń J, Dałek J, Musiał W. The influence of selected factors on the aqueouscryptotanshinone solubility. Pharmaceutics 2021;13(07):992
10 Zhang J, Huang M, Guan S, et al. A mechanistic study of the intestinal absorption of cryptotanshinone, the major active constituent of Salvia miltiorrhiza. J Pharmacol Exp Ther 2006;317 (03):1285–1294

11 Xue M, Cui Y, Wang HQ, Hu ZH, Zhang B. Reversed-phase liquid chromatographic determination of cryptotanshinone and its active metabolite in pig plasma and urine. J Pharm Biomed Anal 1999;21(01):207–213
12 Li H. Design and Synthesis of Cryptotanshinone Derivatives and Their Effects on the Transcriptional Activity of STAT3 [In Chinese]. Fuzhou: Fujian University of Traditional Chinese Medicine; 2021
13 Ding C, Li J, Jiao M, Zhang A. Catalyst-free sp3 C-H acyloxylation: regioselective synthesis of 1-acyloxy derivatives of the natural product tanshinone IIA. J Nat Prod 2016;79(10):2514–2520
14 Liang B, Yu SJ, Li J, et al. Site-selective Csp3-H aryloxylation of natural product tanshinone IIA and its analogues. Tetrahedron Lett 2017;58(19):1822–1825
15 Zhou JH. Synthesis and Vasodilative Activity of cryptotanshinone Derivatives [In Chinese]. Zhengzhou: Zhengzhou University; 2019
16 Meng FF. Synthesis and Cardioprotective Activity Screening Research of Cryptotanshinone Derivatives [In Chinese]. Zhengzhou: Zhengzhou University; 2021
17 Yan L. Cryptotanshinone Suppresses Triple Negative Breast Cancer via Ferroptosis [In Chinese]. Shanghai: Naval Medical University; 2021